DEVELOPMENTAL BIOLOGY

Compliant substratum guides endothelial commitment from human pluripotent stem cells

Quinton Smith,[1] Xin Yi Chan,[1] Ana Maria Carmo,[1] Michelle Trempel,[1] Michael Saunders,[1] Sharon Gerecht[1,2]*

The role of mechanical regulation in driving human induced pluripotent stem cell (hiPSC) differentiation has been minimally explored. Although endothelial cell (EC) fate from hiPSCs has been demonstrated using small molecules to drive mesoderm induction, the effects of substrate stiffness with regard to EC differentiation efficiency have yet to be elucidated. We hypothesized that substrate compliance can modulate mesoderm differentiation kinetics from hiPSCs and affect downstream EC commitment. To this end, we used polydimethylsiloxane (PDMS)—a transparent, biocompatible elastomeric material—as a substrate to study EC commitment of hiPSCs using a stepwise differentiation scheme. Using physiologically stiff (1.7 MPa) and soft (3 kPa) PDMS substrates, compared to polystyrene plates (3 GPa), we demonstrate that mechanical priming during mesoderm induction activates the Yes-associated protein and drives Wnt/β-catenin signaling. When mesoderm differentiation was induced on compliant PDMS substrates in both serum and serum-free E6 medium, mesodermal genetic signatures (*T*, *KDR*, *MESP-1*, *GATA-2*, and *SNAIL-1*) were enhanced. Furthermore, examination of EC fate following stiffness priming revealed that compliant substrates robustly improve EC commitment through VECad, CD31, vWF, and eNOS marker expression. Overall, we show that substrate compliance guides EC fate by enhancing mesoderm induction through Wnt activation without the addition of small molecules. These findings are the first to show that the mechanical context of the differentiation niche can be as potent as chemical cues in driving EC identity from hiPSCs.

INTRODUCTION

A critical hurdle in the promise of regenerative medicine is the ability to robustly generate functional, immune-compatible, vascularized constructs for therapeutic application, acting to replace or augment diseased tissue in vivo (*1*). The advent of human induced pluripotent stem cell (hiPSC) technology has led to renewable sources of patient-specific cells; however, approaches to efficiently guide their maturation to functional vascular lineages in vitro still remain elusive. Key determinants of functioning vasculature in vivo are endothelial cells (ECs), which line blood vessels, acting to mediate the exchange of oxygen, nutrients, and waste from surrounding tissue.

Developmentally, hemangioblasts or precursor cells that give rise to both blood and ECs reside in the lateral plate mesoderm, a process that relies on physiochemical cues to drive mesoderm identity and segmentation from endoderm and ectoderm germ layers. Migration, resulting from epithelial-to-mesenchymal transition (EMT), coincides with stimulus of bone morphogenetic proteins (BMPs), fibroblast growth factors (FGFs), and wingless/INT proteins (Wnts) (*2*). Wnts specifically orchestrate gene expression in a mechanically dependent manner, driving signaling events and changes in cytoskeleton tension by regulating actomyosin activity (*3*).

Mesoderm/primitive streak identity is first established by transcription factor Brachyury (*T*) expression (*4*). Next, lateral plate hemangioblast identity from mesodermal precursors is established by EMT segmentation events regulated by *SNAIL-1* expression (*5*). Subsequently, the transient expressions of insert kinase domain receptor (*KDR*) (*6*), zinc finger transcription factor *GATA-2* (*7*), and transcription factor mesoderm posterior 1 (*MESP-1*) are induced, giving rise to both cardiac and hematopoietic lineages (*8*). Hence, activation of these genetic landmarks through supplementation of BMPs, FGFs and modulation of Wnt during mesoderm induction in vitro has led to successful EC differentiation from hiPSCs with varying efficiency (table S1) (*9*–*14*). One powerful approach is based on the need of canonical Wnt signaling in mesoderm induction, where Wnt drives the accumulation of nuclear β-catenin that binds to T cell factor/lymphoid enhancer factor transcription factors, activating the expression of target genes such as *T* (*15*, *16*).

To this end, glycogen synthase kinase 3 inhibition is used in differentiation protocols to prevent β-catenin degradation to drive mesoderm induction, thereby enhancing EC commitment. While Yes-associated protein/transcriptional coactivator with PDZ binding motif (YAP/TAZ) signaling has been implicated as a sensor of tissue mechanics, where the degree of cell spreading transcriptionally regulates the activity of YAP/TAZ (*17*–*21*). Wnt/β-catenin activity has also been shown to be influenced by mechanical cues (*22*, *23*).

We investigated the role of substrate compliance in EC differentiation by tracking gene expression, along with β-catenin and YAP localization during mesoderm induction. Additionally, we appraised the effects of stiffness-primed mesoderm induction on endothelial fate from hiPSCs through flow cytometry and immunofluorescence staining. Here, we use our previously established stepwise adherent differentiation scheme, which results in early vascular cells (EVCs) consisting of vascular endothelial cadherin–positive ($VECad^+$) (early ECs) and platelet-derived growth factor receptor–β^+ ($PDGFR\text{-}\beta^+$) cells (early pericytes) (*24*). We find that compliant substrates enhance not only mesodermal commitment but also endothelial specification. Moreover, serum-free, well-defined minimalistic E6 medium, without the addition of small molecules, enhances endothelial fate, which is further increased when compliant substrates are used during mesoderm induction. Overall, we describe for the first time a robust approach to direct mesoderm differentiation without directly manipulating Wnt signaling with small molecules but by leveraging mechanical cues.

[1]Department of Chemical and Biomolecular Engineering and Institute for NanoBioTechnology, Johns Hopkins University, Baltimore, MD 21218, USA. [2]Department of Materials Science and Engineering, Johns Hopkins University, Baltimore, MD 21218, USA.
*Corresponding author. Email: gerecht@jhu.edu

RESULTS

Compliant substrates for direct hiPSC differentiation

Inspired by developmental cues, we aimed to study how stiffness modulates hiPSC differentiation toward endothelial fate. To eliminate occasions of spontaneous tube formation and enable control over cell attachment and spreading, we sought to use elastomeric-based substrates. We fabricated biocompatible substrates that span physiologically relevant stiffness by changing the ratio between commercially available polydimethylsiloxane (PDMS) elastomer base to curing agent. To create physiologically stiff PDMS substrates, we generated substrates with a Young's modulus (E) of ~1.7 ± 0.2 MPa, ~0.6 ± 0.5 MPa, and ~50 ± 1.3 kPa (fig. S1). However, using these substrates in initial studies resulted in minimal changes in mesodermal induction or endothelial specification. To this end, we broadened the stiffness range and fabricated physiologically soft PDMS-based gels with E ~ 3 kPa, as previously described (*25*).

Wettability was tested across physiologically stiff and soft compliant silicone substrates, and they were shown to be hydrophobic before collagen IV coating. Subsequent to coating, we observed an increase in hydrophilicity, evidenced by a decrease in the contact angle. Whereas the surface energies of the PDMS substrates were not significantly different before and after coating, polystyrene-coated surfaces with E ~ 3 GPa showed significantly higher hydrophilicity after collagen coating (Fig. 1, A and B). Fourier transform infrared spectroscopy (FTIR) confirmed consistency in PDMS chemical composition across E ~ 1.7 MPa and E ~ 3 kPa substrates, in the presence and absence of collagen IV (Fig. 1C). We next seeded hiPSCs on substrates ranging in compliance for 24 hours at a sparse density to observe YAP localization as a function of stiffness.

We observed similar attachment across PDMS and E ~ 3 GPa substrates (Fig. 1D), where YAP was activated and primarily localized in the nucleus on E ~ 3 GPa substrates (96 ± 5%), that steadily became cytoplasmic and deactivated on E ~ 1.7 MPa (73 ± 3%) and E ~ 3 kPa (48 ± 2%) substrates, corresponding to the degree of spreading (Fig. 1, E and F).

Stiffness-dependent YAP/β-catenin localization during mesoderm induction

To determine the degree of Wnt/β-catenin signaling along hiPSC-mesodermal induction, we tracked the localization of YAP and β-catenin in confluent differentiation cultures optimized to induce EVCs (*26*). The ratio of nuclear to cytoplasmic YAP was significantly higher on PDMS substrates in comparison to E ~ 3 GPa substrates throughout mesoderm induction, suggesting Wnt activation (Fig. 2A). To confirm the consequence of increased nuclear YAP along mesoderm induction on PDMS substrates, we next monitored the localization of β-catenin. We found that on day 2 of differentiation, β-catenin expression was higher and primarily localized at cell-cell junctions on E ~ 1.7 MPa and E ~ 3 kPa substrates. In comparison, the expression of β-catenin on E ~ 3 GPa was considerably reduced. By day 4 of differentiation, the cytoplasmic pool of β-catenin increased and was subsequently degraded by day 6 of differentiation on PDMS substrates. On day 4 of differentiation on E ~ 3 GPa, β-catenin remained diffuse but became stabilized at cell-cell junctions by day 6 (Fig. 2B). When comparing the kinetics of β-catenin and YAP localization, we found that an increased junctional pool of β-catenin was rapidly shuttled on E ~ 1.7 MPa and E ~ 3 kPa substrates. Conversely, E ~ 3 GPa surfaces had little β-catenin activity at days 2 and 4 of differentiation, accompanied by the reestablishment of junctional β-catenin by day 6. YAP activity was significantly higher on PDMS substrates when compared to E ~ 3 GPa surfaces throughout the entirety of differentiation (Fig. 2C). Although YAP nuclear activity remained relatively constant throughout mesoderm induction on 1.7-MPa surfaces, a pool of junctionally stable β-catenin accumulated cytoplasmically by day 6 of mesoderm induction. These characteristics were mirrored on 3-kPa substrates, with YAP activity increasing on day 4, followed by a reduction by day 6. Collectively, these results suggest that compliant substrates activate the release of stabilized β-catenin toward the cytoplasm, where it can coordinate Wnt-specific mesoderm transcriptional activity.

Compliant substrates enhance mesoderm induction and endothelial commitment

After establishing the kinetics of YAP and β-catenin localization along mesoderm induction on varied substrate stiffness, we next accessed whether the altered shuttling influenced mesodermal gene expression and downstream EC specification according to our differentiation scheme (Fig. 3A). To study the kinetics of early differentiation events in vitro as a function of substrate stiffness, we first documented that cells did not exhibit biased attachment or proliferation on the collagen IV–coated substrates in serum-containing medium (fig. S2). We next probed whether the physical properties of the underlying substrate had any consequences on mesoderm induction and specification in the differentiation medium. We verified that under all substrates tested, cells rapidly lost *OCT-4* expression and were no longer pluripotent by day 6 (fig. S2). We next monitored gene expression along the mesodermal induction step and found up-regulation of *T*, *KDR*, *MESP-1*, and *SNAIL-1* when hiPSCs were differentiated on compliant substrates, whereas *GATA-2* was up-regulated only on E ~ 3 kPa (Fig. 3B). Moreover, the expression of *T* peaked on day 2 (day 4 on 3-kPa substratum), followed by peak expression of *MESP-1* and *GATA-2* on day 4, whereas *KDR* and *SNAIL-1* expression peaked on day 6 of the mesodermal induction period. Overall, these results suggest that mesoderm induction is sensitive to substrate stiffness, with a consistent up-regulation of mesodermal genes on compliant PDMS substrates in comparison to E ~ 3 GPa substrates.

Next, we hypothesized that the enhanced mesodermal induction, primed through culture on compliant PDMS substrates, could influence the capacity of hiPSCs to undergo endothelial fate. Toward this, mechanically primed mesoderm-induced cells were replated on E ~ 3 GPa plates for EC derivation according to our two-step differentiation scheme. By day 12 of differentiation, we identified morphological differences in our EVC populations, dependent on the substrate used during mesoderm induction. When EVCs were differentiated continuously on E ~ 3 GPa polystyrene plates, no distinct morphological differences could be observed. In contrast, EVCs primed on E ~ 1.7 MPa and E ~ 3 kPa substrates displayed areas of distinct cobblestone-forming cells (Fig. 3C), surrounded by elongated cell bundles, as previously described (*26*, *27*). Examining vascular commitment, we could not observe differences in PDGFR-β expression among the different stiffness substrates from flow cytometry (fig. S3). EVCs primed on E ~ 3 GPa had similar cumulative expression of VECad when compared to EVCs derived using PDMS substrate priming. However, the generated populations from PDMS substrates contained two distinct high VECad– and low VECad–expressing populations, as compared to human umbilical vein endothelial cells (HUVECs) (Fig. 3D). Because flow cytometry is sensitive in detecting low-expressing populations, we validated VECad expression based on substrate stiffness through immunofluorescence staining. Although VECad expression could be detected through flow

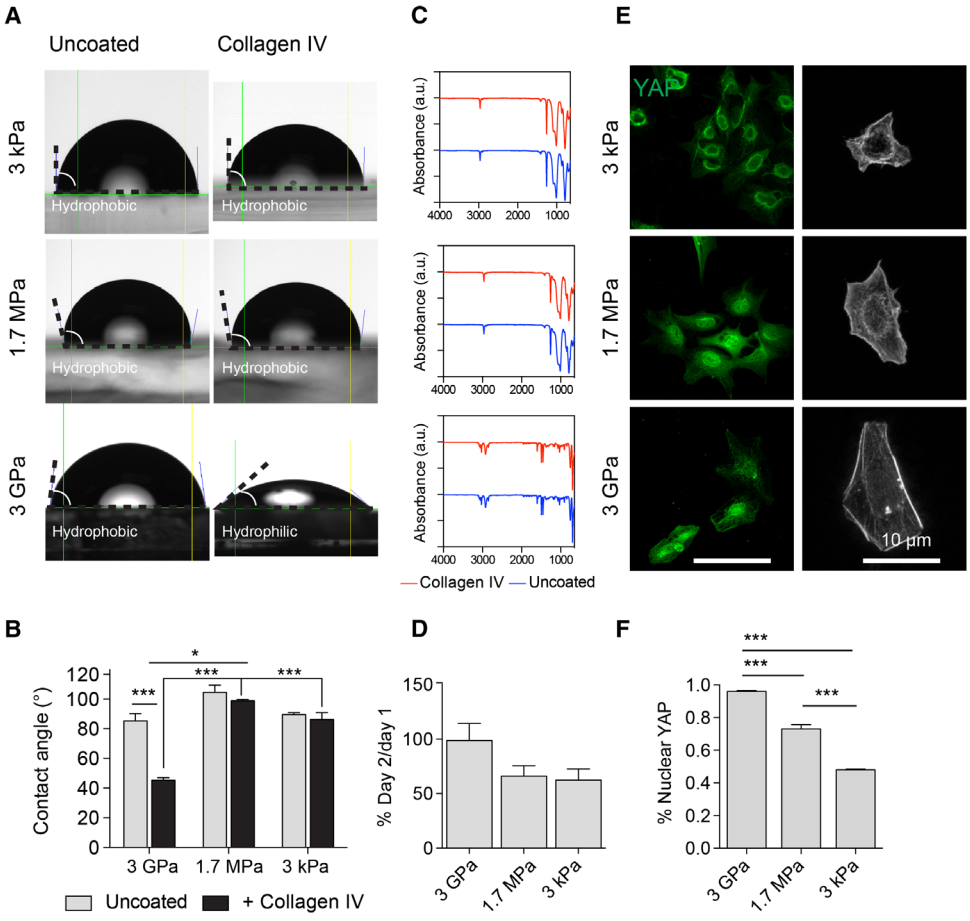

Fig. 1. PDMS substrates are permissive to hiPSC differentiation. (**A**) Representative images of water droplets on collagen IV–coated and uncoated PDMS and *E* ~ 3 GPa substrates for contact angle measurements. (**B**) Contact angle quantification across substrates. (**C**) FTIR analysis of substrates with and without collagen IV coating. a.u., arbitrary units. (**D**) Attachment efficiency across substrates. (**E**) Sparse seeding elicits varied YAP (green) localization and spreading [filamentous actin (F-actin) in gray] dependent on substrates with corresponding (**F**) quantification. All data are presented as means ± SEM. *P < 0.05; **P < 0.01; ***P < 0.001. At least three replicates were performed.

cytometry in ECs derived from *E* ~ 3 GPa, only a small subset of the population could be identified through immunohistochemistry (Fig. 3E). To further analyze endothelial commitment and maturation, we stained day 12 EVCs with a series of mature EC markers. In agreement with our previous publication (*24*), we found that EVCs derived from *E* ~ 3 GPa contained ECs that were nascent, lacking mature von Willebrand factor (vWF) and endothelial nitric oxide synthase (eNOS) marker expression. On the contrary, EVCs derived from compliant PDMS substrates contained ECs that expressed not only VECad and CD31 in abundance but also occasional eNOS and punctate vWF localization (fig. S4). Collectively, these results suggest that the degree of mesoderm induction influences the capacity for downstream endothelial differentiation and maturation.

Compliant substrates enhance serum-free, cytokine-free mesoderm induction and subsequent endothelial maturation

The use of animal-derived products in the differentiation medium leads to inherent variability during differentiation (*14*). To address this problem, we adapted our mesoderm induction scheme to serum-free, chemically defined conditions using minimalistic medium consisting of Dulbecco's modified Eagle's medium (DMEM)/F12, sodium bicarbonate, selenium, ascorbic acid, transferrin, and insulin (that is, E6 medium) (Fig. 4A). We observed enhanced attachment and proliferation across all substrates. Specifically, compared to hiPSCs differentiated using medium containing serum (see fig. S2), hiPSCs differentiated in E6 medium contained 156 ± 39% of the seeded population and proliferated rapidly, reaching 4.46 times the initial cell-seeding density (fig. S5). We found enhanced expression of *T* and *SNAIL-1* on compliant substrates compared to *E* ~ 3 GPa substrates, whereas *GATA-2* expression was up-regulated on *E* ~ 3 kPa compared to *E* ~ 3 GPa substrates. We found an earlier peak in the expression of *SNAIL-1*, *KDR*, and *GATA-2* on both compliant PDMS substrates compared to the serum-containing medium conditions, suggesting an earlier onset of mesodermal differentiation and EMT toward the vascular lineage (Fig. 4B). This data set is the first to reveal that differentiating hiPSCs undergo rapid proliferation under serum-free conditions and can undergo enriched mesoderm specification, without the need for additional small molecules.

Regardless of the substrate used, we consistently observed enriched mesoderm through mRNA expression from E6 medium conditions and typically saw enhanced endothelial differentiation efficiency with our differentiation protocol. It should be noted that initial studies on *E* ~ 3 GPa substrates showed an increase in VECad expression when

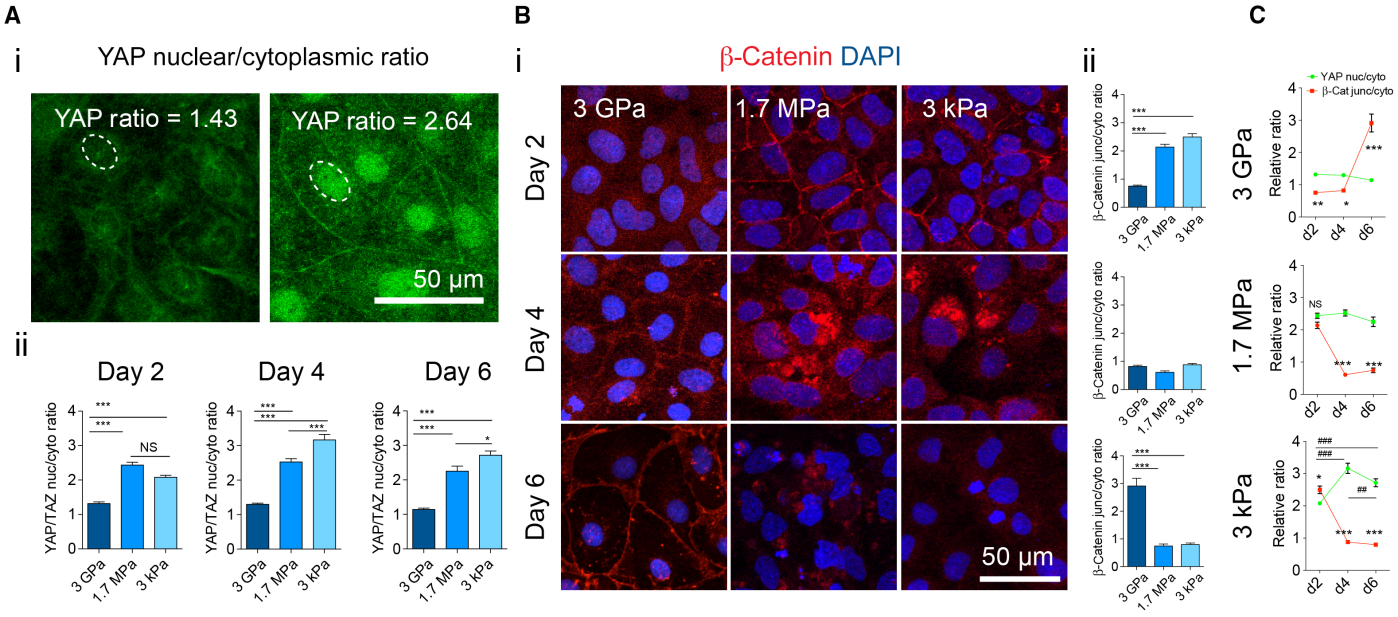

Fig. 2. YAP/β-catenin signaling as a function of substrate stiffness along mesoderm induction. (**A**) (i) Sample of image quantification of the ratio between nuclear and cytoplasmic YAP intensity. (ii) YAP nuclear-to-cytoplasmic (nuc/cyto) ratios on days 2, 4, and 6 of differentiation on the various substrates. NS, not significant. (**B**) (i) Representative immunofluorescence images (red, β-catenin; blue, nuclei) and (ii) quantification of the junctional-to-cytosolic (junc/cyto) ratio of β-catenin expression on days 2, 4, and 6 of differentiation on the various substrates. DAPI, 4′,6-diamidino-2-phenylindole. (**C**) Comparison between YAP (green) and β-catenin (red) localization as a function of time on the various substrates (comparison between relative YAP and β-catenin localization reported as *; changes in the relative YAP nuclear-to-cytoplasmic ratio across days of differentiation reported as #). Data are represented as means ± SEM. $^{*/\#}P < 0.05$, $^{**/\#\#}P < 0.01$, $^{***/\#\#\#}P < 0.001$, two-way analysis of variance (ANOVA). At least three biological replicates were performed.

using E6 for the mesoderm induction stage. After switching stiffness-primed, serum-free mesodermal cells to $E \sim 3$ GPa and continuing differentiation under vascular endothelial growth factor (VEGF) stimulation, we found that under all differentiation conditions, cobblestone-like colonies were formed (Fig. 4C). The population of high VECad–expressing cells was increased in comparison to serum containing differentiation conditions, with significantly higher expression on compliance substrates, reaching ~75% on $E \sim 1.7$ MPa substrates (Fig. 4, D and E, i). Remarkably, VECad expression gated at intensity levels correlating with HUVECs was significantly higher in populations primed on compliant PDMS substrates (Fig. 4E, ii), with insignificant differences in PDGFR-β expression between differentiation conditions (fig. S6). We found that on $E \sim 1.7$ MPa substrates, VECad and CD31 were abundantly expressed (fig. S7), with corresponding eNOS and punctate vWF expression in comparison to $E \sim 3$ GPa primed surfaces (Fig. 4E and fig. S8). Collectively, these results show that serum-free differentiation, in conjunction with compliant substrate mesoderm induction, directs EC differentiation efficiency and mature marker expression.

DISCUSSION

Although adult endothelial progenitor populations, such as endothelial colony-forming cells, are highly proliferative and show promise for treating patients with vascular disorders by homing to sites of injury, their availability in vivo and expansion in vitro are limited. As a result, patient-derived hiPSCs, which have the unique capacity of unlimited self-renewal and ability to mature into all cell types in the body, pose as a renewable source of therapeutic ECs. Currently, methods for deriving ECs from hiPSCs rely mainly on chemical signals, although mechanical cues have been shown to be essential for morphogenetic events and tissue organization during embryonic development. For example, cues exerted from the extracellular matrix (ECM) can induce tensile forces that drive early cell polarity events as well as lineage specification during differentiation (*28*–*30*). To this end, we investigated the effects of substrate mechanics on EC differentiation using a genetically sequenced hiPSC line (BC1), whose derivation was achieved with non-viral reprogramming.

Before studying the effects of substrate mechanics on hiPSC differentiation, we assessed the reproducibility and ease of manipulation of several biomaterials. Utilization of PDMS in soft lithography has led to its widespread adoption in microfluidic and lab-on-a-chip technologies, although its use in basic science remains limited in spite of its ease of manipulation. In addition to its low cost, optical properties, and biocompatibility, PDMS is an attractive biomaterial in that its E can be tuned. Hence, there is an opportunity to demonstrate the utility of PDMS as a suitable biomaterial to study mechanical cues in controlled in vitro stem cell differentiation. In spite of its hydrophobicity, which can influence the degree of ECM protein absorption (*31*), we found PDMS as a suitable candidate because of its lack of swelling in aqueous environments and prolonged maintenance of elasticity under culture conditions.

In the absence of Wnt signaling, YAP is cytoplasmically localized, aiding in the destruction of β-catenin, whereas in the presence of Wnt signaling, YAP and β-catenin become transcriptionally active (*32*). The observation that YAP/TAZ nuclear exclusion is dependent on substrate stiffness is a phenotype that is also dependent on cell density and ECM availability (*19*, *33*). On the other hand, it is well established that initial cell-seeding density of hiPSCs is crucial to differentiation outcome and has been demonstrated in several lineages arising from mesodermal progenitors including cardiomyocytes, epithelial cells, and

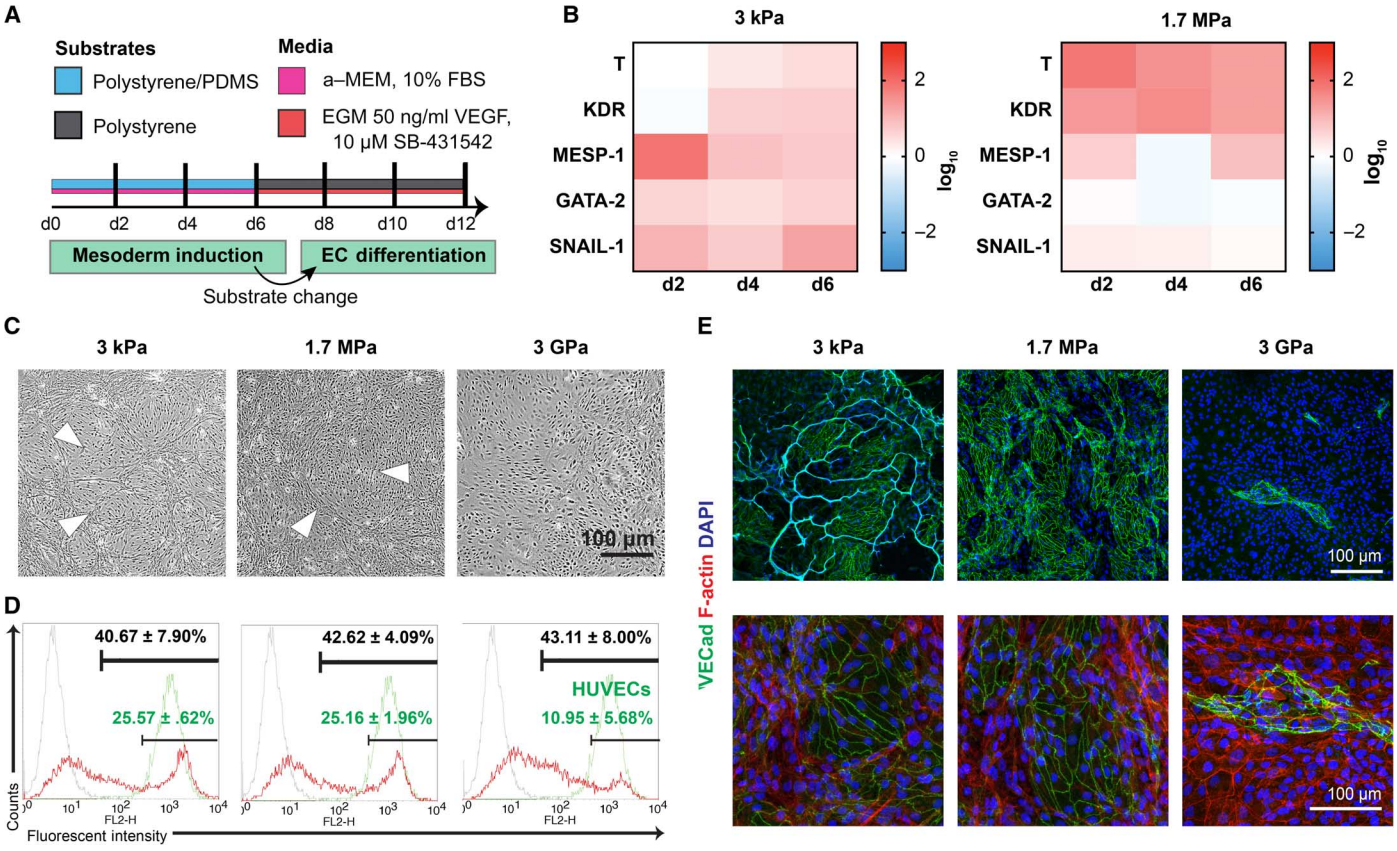

Fig. 3. Stiffness-primed mesoderm induction in the presence of serum enhances EC differentiation. (**A**) Schematic of stiffness-primed mesoderm induction followed by EC differentiation on *E* ~ 3 GPa substrates. α-MEM, α-minimum essential medium; FBS, fetal bovine serum; EGM, endothelial growth medium. (**B**) Left: Gene expression of mesodermal markers for cells differentiated on soft 3-kPa substrates, normalized to expression from *E* ~ 3 GPa surfaces. Right: Gene expression analysis of cells differentiated on stiff 1.7-MPa substrates, normalized to expression from *E* ~ 3 GPa surfaces. Color key is presented in $\log_{10}$ scale. (**C**) Bright-field images of cobblestone endothelial colonies (white arrows) on day 12 EVCs. (**D**) Day 12 EVC flow cytometry plots of VECad expression in red, with corresponding HUVEC VECad expression in green. Black font, VECad$^+$ cells; green font, highly expressing VECad$^+$ cells. Data are presented as means ± SEM. (**E**) Representative immunofluorescence images of VECad expression on day 12 EVCs: Low-magnification (top) and high-magnification (bottom) images are shown (green, VECad; red, phalloidin; blue, nuclei). At least three biological replicates were performed.

ECs (*34*–*36*). Dupont *et al.* (*17*) showed that the degree of cell spreading and substrate compliance regulates localization and transcriptional activity of YAP/TAZ. When mature or stem cells were grown on soft substrates or geometrically confined micropatterns (both of which limit their spreading), endogenous YAP was excluded from the nucleus. These observations were opposite in cells grown on stiff substrates or patterns that allowed cell spreading (*17*, *19*).

In concordance with these reports, we find that in the absence of cell-cell contacts, YAP localization in hiPSCs is stiffness-dependent (see Fig. 1). However, aiming to probe the role of substrate compliance on mesoderm induction and downstream endothelial specification, we used our differentiation scheme requiring dense seeding for robust differentiation (*26*). Under these culture conditions, cell-cell contact is an additional mechanoregulatory signal contributing to the stimuli provided by the mechanical properties of the underlying substratum. Despite similar attachment and growth rates 6 days after differentiation, we find the YAP localization is cytoplasmic on *E* ~ 3 GPa, with primary nuclear localization on *E* ~ 1.7 MPa and *E* ~ 3 kPa PDMS substrates. We suspect that this discrepancy in YAP localization on *E* ~ 3 GPa substrates correlates to the seeding density used in our differentiation protocol, which is substantiated in other in vitro systems, where YAP is cytoplasmically constrained in dense culture (*37*). Furthermore, YAP localization not only is regulated by substrate stiffness but also acts as a downstream effector of the Hippo pathway network, which is implicated in cell proliferation, apoptosis, and transcriptional events that control differentiation (*18*).

In a previous study, we demonstrated that mesoderm induction under hypoxic conditions is more potent in biasing endothelial fate than hypoxic culture after mesoderm induction (*27*). This observation that early differentiation cues are important in priming downstream endothelial specification has been substantiated further (*12*, *27*, *36*, *38*, *39*). Thus, we focused on the role of substrate stiffness during early differentiation time points. In relation to substrate stiffness, Azzolin *et al.* (*32*) demonstrate that in a "Wnt on" state, YAP dissociates from the β-catenin destruction complex, promoting its transcriptional responses. Thus, we speculated that the cytoplasmic retention of YAP during mesoderm induction on *E* ~ 3 GPa substrates represents a "Wnt off" state corresponding to a suppression of β-catenin nuclear activity, where it can act on target genes such as *T* (*15*, *32*). We found an up-regulation of an array of mesodermal markers, including *T*, at the mRNA level on hiPSCs differentiated on compliant substrates, in comparison to *E* ~ 3 GPa polystyrene plates. This work suggests that substrate rigidity can

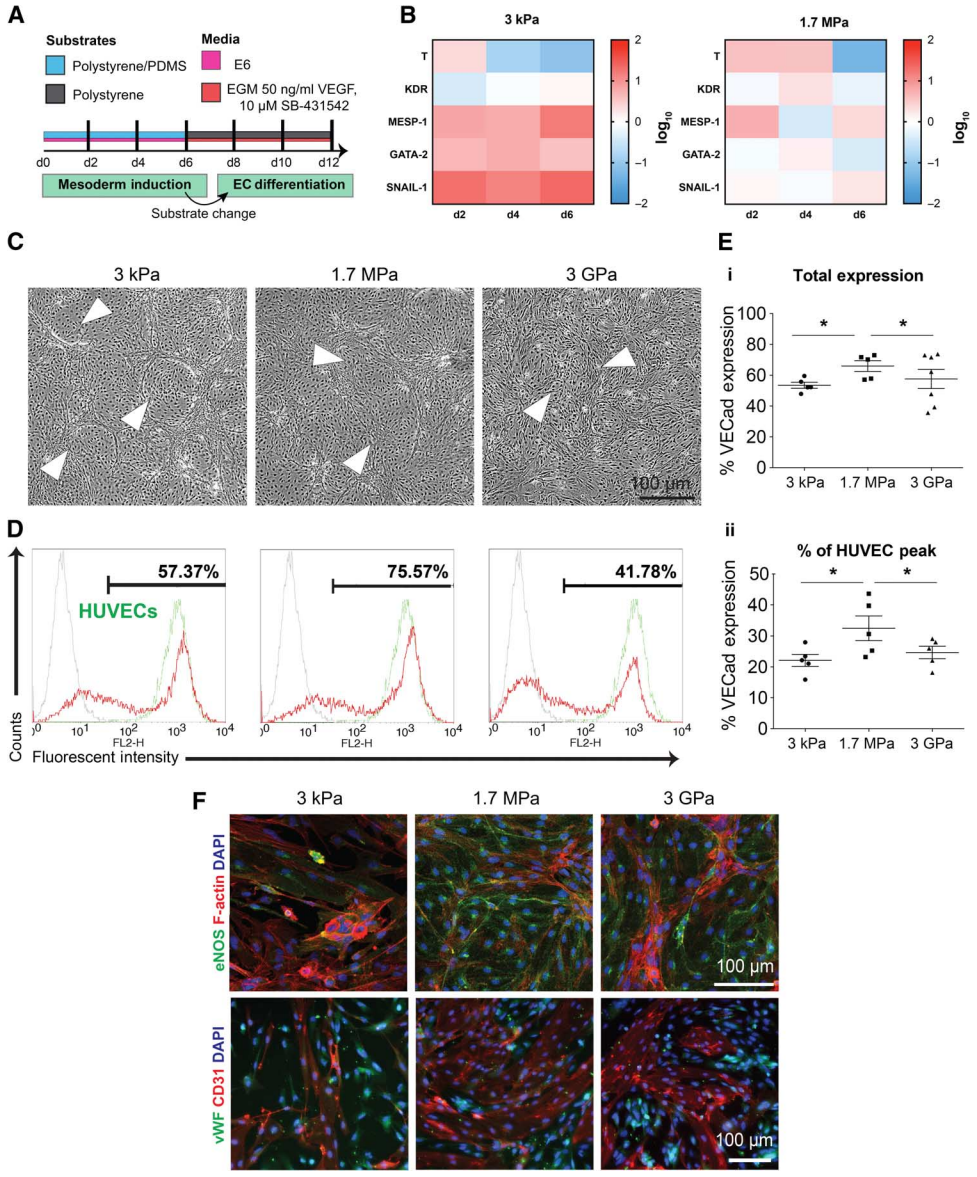

Fig. 4. Stiffness-primed mesoderm induction in serum-free conditions results in robust EC differentiation. (**A**) Schematic of stiffness-primed mesoderm induction followed by EC differentiation on polystyrene plates. (**B**) Left: Gene expression of mesodermal markers for cells differentiated on soft 3-kPa substrates, normalized to expression from $E \sim 3$ GPa surfaces. Right: Gene expression analysis of cells differentiated on stiff 1.7-MPa substrates, normalized to expression from $E \sim 3$GPa surfaces. Color key is presented in $\log_{10}$ scale. (**C**) Bright-field images of cobblestone endothelial colonies (white arrows) on day 12 EVCs. (**D**) Representative day 12 EVC flow cytometry plots of VECad expression in red, with corresponding HUVEC VECad expression in green. (**E**) (i) Total VECad expression as a function of substrate stiffness. (ii) Percentage of VECad expression relative to HUVEC control samples. (**F**) Representative immunofluorescence images of day 12 EVC expression (top: green, eNOS; red, F-actin; blue, nuclei, bottom: green, vWF; red, CD31; blue, nuclei). Data are represented as means ± SEM. *$P < 0.05$, **$P < 0.01$, and ***$P < 0.001$, paired Student's t test. At least three biological replicates were performed.

enhance mesodermal induction through temporal modulation of Wnt/β-catenin signaling. Comparing serum and chemically defined mesoderm induction, we did not observe significant differences in attachment but did note that differentiating hiPSCs seem to proliferate more under serum-free conditions.

In our stepwise differentiation approach, the mechanically dosed mesoderm populations are switched to $E \sim 3$ GPa polystyrene plates and differentiated in medium permissive to both endothelial and perivascular lineages. We found that EVCs mechanically dosed on either $E \sim 1.7$ MPa or $E \sim 3$ kPa PDMS substrates under both serum or chemically defined conditions undergo enriched endothelial specification without the addition of growth factors or inhibitory molecules during mesoderm induction. This is evidenced by high VECad expression in relation to HUVEC controls. Our results show that stiffness priming under serum-free derivation can result in up to 75% high-expressing VECad$^+$ cells. Using immunofluorescence microscopy, we can positively identify mature endothelial markers vWF and eNOS, without the need for intermediate sorting steps or prolonged culture, as previously described (*24*, *36*), suggesting that substrate compliance accelerates the maturation of endothelial derivatives. Overall,

we harness hiPSCs' ability to sense and interpret substrate stiffness and direct endothelial commitment through canonical Wnt activation. Using elastomeric PDMS substrates, we show that the mechanical context of the differentiation niche can be as potent as chemical cues in driving endothelial identity from hiPSCs. Although we show the temporal enhancement of mesodermal gene expression on compliant substrates under both serum and serum-free conditions, future studies showing the potential of these populations to differentiate into other mesodermal lineages such as cardiomyocytes would help validate our results.

Although there is a wide array of literature on the effects of substrate compliance on mature or multipotent mesenchymal stem cells in vitro, there are limited studies analyzing the behaviors of differentiating hiPSCs in complex, controlled environments. Here, we provide evidence that stiffness drives mesodermal differentiation under serum and serum-free conditions, leading to endothelial commitment. Future studies that further decouple the effects of substrate mechanics and chemical cues by eliminating serum in the medium of the endothelial differentiation step and using synthetic ECM to guide attachment are needed. Moreover, there is an opportunity to further recapitulate development events in vitro through combining compliant mesoderm induction under hypoxic conditions. Overall, our results validate the importance of interdisciplinary approaches in understanding the complex extracellular milieu that controls stem cell differentiation.

MATERIALS AND METHODS

Experimental design

The objective of this study was to evaluate the role of substrate stiffness on the differentiation of ECs from hiPSCs. To this end, we used a stepwise adherent differentiation scheme, which begins with a mesodermal induction period, followed by an endothelial commitment step. We formulated $E \sim 1.7$ MPa and $E \sim 3$ kPa PDMS substrates amenable to cell adhesion and spreading and tracked the localization of the mechanosensitive protein YAP, as well as β-catenin, a known Wnt-modulated factor essential in mesoderm induction. We then analyzed gene expression of mesodermal markers along differentiation under serum and serum- and cytokine-free conditions, compared to differentiation on $E \sim 3$ GPa polystyrene plates. Finally, we appraised the differentiation potential of mechanically primed mesoderm pools, differentiated on either $E \sim 1.7$ MPa or $E \sim 3$ kPa substrates as well as on $E \sim 3$ GPa plates. This was achieved by re-replating on $E \sim 3$ GPa plates for the endothelial commitment step. To evaluate EC differentiation robustness, we used a combination of flow cytometry and immunofluorescence microscopy to denote marker expression and degree of maturation.

Preparation of compliant substrates

For PDMS substrates, 10:1, 20:1, and 50:1 ratios of PDMS to curing agent (Sylgard 184, Dow Corning) were mixed to generate 1.7 ± 0.2 MPa, 0.6 ± 0.5 MPa, and 50 ± 1.3 kPa, respectively. PDMS substrates (3 kPa) were fabricated by mixing silicone and curing agent (CY 52-276A and CY 52-276B, Dow Corning), as previously described (*25*). Elastomeric mixtures were placed into a vacuum desiccator for 2 min to remove air bubbles. Next, the mixed elastomeric solution was pipetted into each well of the tissue culture vessels. For imaging studies, a thin layer of PDMS was coated onto a 35-mm, 14-mm MatTek No. 1.0 cover glass, using a speed of 1000 rpm for 60 s with a 100-rpm acceleration time to spin-coat PDMS substrates. The spin-coated dish was placed on a flat surface and cured for 30 min at 70°C for 3-kPa substrates and for 1 hour at 65°C for the Sylgard 184 surfaces.

Water contact angle measurements

To determine the relative wettability of the substratum used in mesoderm induction, we conducted contact angle measurements for soft and physiologically stiff PDMS substrates and polystyrene plates. Briefly, samples were prepared by sterilization, followed by incubation with collagen IV for 1 hour at room temperature, rinsed with sterile phosphate-buffered saline (PBS), and stored at 4°C before analysis. Water contact angle measurements were conducted using a 260-F4 goniometer from ramé-hart Instrument Co. Several symmetrical water droplets were dispensed onto the substrate for the measurement. The contact angle was then obtained with the DROPimage software using a circular geometry method.

FTIR measurement

Surface functionality on each substrate was analyzed using a Spectrum 100 instrument from PerkinElmer. The test was conducted using an attenuated total reflection mode with a diamond crystal. Scan resolution was 4 cm^{-1}, and scan number was 16. All samples were analyzed in a consistent manner.

hiPSC culture and maintenance

The BC1 hiPSC line was provided by L. Cheng (*40*). This hiPSC line was maintained on an inactivated mouse embryonic fibroblast (MEF) feeder layer supplemented with 80% ES-DMEM/F12 and 20% knockout serum on tissue culture plates at 5% CO_2 and 37°C. Cell medium was replaced every day. Cells were passaged using collagenase type IV (1 mg/ml; Invitrogen). hiPSCs were routinely examined for pluripotent markers using immunofluorescence staining and flow cytometry analysis for TRA-1-60, TRA-1-81, SSEA-4, and OCT-4.

Early vascular differentiation on different substrates

Differentiation followed our previous published protocol (*24*, *26*, *38*). hiPSCs were collected through digestion with EDTA (Promega) and separated into a single-cell suspension using a 40-μm mesh strainer (BD Biosciences). The single cells were plated onto collagen IV (Corning)–coated plates or PDMS substrates at 1×10^5 cells/cm^2 with 10 μM ROCK inhibitor Y-27632 (STEMCELL Technologies). During mesodermal induction, cells were cultured in a differentiation medium composed of α-MEM (Invitrogen), 10% FBS (HyClone), and 0.1 mM β-mercaptoethanol, as previously described. Differentiation medium was changed every other day for a total of 6 days. In early vascular differentiation, day 6 mesodermal cells were digested and collected with TrypLE Express (Invitrogen), strained, and seeded on fresh collagen IV plates at 3×10^4 cells/cm^2 in EC differentiation medium composed of EGM (PromoCell) supplemented with 10 μM transforming growth factor–β inhibitor SB-431542 (Tocris), VEGF (50 ng/ml), 2% FBS, and 0.1% penicillin-streptomycin. The medium was changed every other day for an additional 6 days. In the serum-free mesodermal differentiation protocol, E6 medium (Life Technologies) was used in place of the α-MEM–based differentiation medium. On day 12, light microscopy was used to identify morphological differences in the resulting differentiated populations. In addition, cells were collected for flow cytometry analysis or fixed for immunofluorescence staining.

Flow cytometry

Flow cytometry was performed as previously described (*24*, *26*, *27*, *38*). Briefly, cells were incubated with phycoerythrin-conjugated antigen-specific antibodies for markers outlined in the text. All analyses were

done using the corresponding isotype or no stain controls. Forward/side scatter plots were used to exclude dead cells. User guide instructions were followed to complete the flow cytometry analysis via the CellQuest Pro software (BD Biosciences).

Immunofluorescence and imaging

Differentiated EVCs were prepared for immunofluorescence, as previously shown (*24*, *26*, *27*). Briefly, cells were fixed using 3.7% paraformaldehyde for 5 to 10 min at room temperature and washed three times using PBS. The fixed cells were permeabilized with 0.1% Triton X-100 for 10 min and incubated with 1% bovine serum albumin blocking solution at room temperature for 1 hour. Samples were incubated with either the antigen-specific primary antibodies for the markers outlined in the text, followed by appropriate secondary antibodies (table S2), or with phalloidin (1:500; Molecular Probes) and DAPI (1:10,000; Molecular Probes). Both primary and secondary antibodies were diluted in an antibody diluent (Dako). The immunolabeled cells were imaged using a confocal microscope (Zeiss LSM 780). Quantification of nuclear to cytoplasmic YAP and junctional to cytosolic β-catenin was performed as previously described (*20*) for $n > 25$ cells per condition.

Quantitative reverse transcription polymerase chain reaction gene expression analysis

Total RNA was isolated from individual samples, along the 6-day mesoderm induction period at time points indicated throughout the text using TRIzol reagent (Invitrogen), and the RNA quality was examined with NanoDrop. Pluripotent stem cells maintained on MEF were collected before each differentiation experiment to ascertain basal levels of the aforementioned mesodermal markers and served as a control to monitor maturation. Complementary DNA (cDNA) library was generated using 1 μg of high-quality total RNA using Moloney murine leukemia virus reverse transcriptase (Promega) and oligo(dT) primers (Promega) as per the manufacturer's instructions. The specific assay used was the TaqMan Universal PCR Master Mix and Gene Expression Assay (Applied Biosystems) for OCT-4, T, GATA-2, SNAIL-1, MESP-1, and GAPDH as per the manufacturer's instructions. The TaqMan PCR step was performed with an Applied Biosystems StepOne Real-Time PCR System. The relative expressions of the genes were normalized to the amount of endogenous control GAPDH in the same cDNA by using the standard curve method provided by the manufacturer. For each primer set, the comparative computerized tomography method (Applied Biosystems) was used to calculate the amplification differences between the different samples. The values for the experiments were averaged and graphed with SDs.

Statistical analysis

All analyses were performed in at least biological triplicates. Two-tailed *t* test was performed to determine significance. All graphs were drawn using GraphPad Prism 6. Significance levels were set at $*P < 0.05$, $**P < 0.01$, $***P < 0.001$, and $****P < 0.0001$.

SUPPLEMENTARY MATERIALS

Supplementary material for this article is available at http://advances.sciencemag.org/cgi/content/full/3/5/e1602883/DC1

fig. S1. Development of compliant PDMS substrates.
fig. S2. Differentiation and proliferation are supported on compliant silicone substrates.
fig. S3. PDGFR-β expression from mesodermal differentiation in serum.
fig. S4. Immunofluorescence microscopy of mature EC markers after mesoderm stiffness priming.
fig. S5. Differentiation and proliferation are supported on compliant silicone substrates in serum-free conditions.
fig. S6. PDGFR-β expression from mesodermal differentiation in serum-free conditions.
fig. S7. Immunofluorescence microscopy of EC markers after chemically defined mesoderm stiffness priming.
fig. S8. Immunofluorescence microscopy of EC markers after chemically defined mesoderm stiffness priming.
table S1. Literature review of techniques to induce mesodermal specification from hiPSCs.
table S2. Antibodies used in this study.
References (*41*, *42*)

REFERENCES AND NOTES

1. A. Khademhosseini, R. Langer, A decade of progress in tissue engineering. *Nat. Protoc.* **11**, 1775–1781 (2016).
2. C. L. Mummery, J. Zhang, E. S. Ng, D. A. Elliott, A. G. Elefanty, T. J. Kamp, Differentiation of human embryonic stem cells and induced pluripotent stem cells to cardiomyocytes: A methods overview. *Circ. Res.* **111**, 344–358 (2012).
3. T. Mammoto, D. E. Ingber, Mechanical control of tissue and organ development. *Development* **137**, 1407–1420 (2010).
4. T. Brunet, A. Bouclet, P. Ahmadi, D. Mitrossilis, B. Driquez, A.-C. Brunet, L. Henry, F. Serman, G. Béalle, C. Ménager, F. Dumas-Bouchiat, D. Givord, C. Yanicostas, D. Le-Roy, N. M. Dempsey, A. Plessis, E. Farge, Evolutionary conservation of early mesoderm specification by mechanotransduction in Bilateria. *Nat. Commun.* **4**, 2821 (2013).
5. M. A. Nieto, The snail superfamily of zinc-finger transcription factors. *Nat. Rev. Mol. Cell Biol.* **3**, 155–166 (2002).
6. J. Y. Tan, G. Sriram, A. J. Rufaihah, K. G. Neoh, T. Cao, Efficient derivation of lateral plate and paraxial mesoderm subtypes from human embryonic stem cells through GSKi-mediated differentiation. *Stem Cells Dev.* **22**, 1893–1906 (2013).
7. M. Maeno, P. E. Mead, C. Kelley, R.-h. Xu, H.-f. Kung, A. Suzuki, N. Ueno, L. I. Zon, The role of BMP-4 and GATA-2 in the induction and differentiation of hematopoietic mesoderm in Xenopus laevis. *Blood* **88**, 1965–1972 (1996).
8. S. S.-K. Chan, X. Shi, A. Toyama, R. W. Arpke, A. Dandapat, M. Iacovino, J. Kang, G. Le, H. R. Hagen, D. J. Garry, M. Kyba, Mesp1 patterns mesoderm into cardiac, hematopoietic, or skeletal myogenic progenitors in a context-dependent manner. *Cell Stem Cell* **12**, 587–601 (2013).
9. S. Levenberg, J. S. Golub, M. Amit, J. Itskovitz-Eldor, R. Langer, Endothelial cells derived from human embryonic stem cells. *Proc. Natl. Acad. Sci. U.S.A.* **99**, 4391–4396 (2002).
10. S. Levenberg, L. S. Ferreira, L. Chen-Konak, T. P. Kraehenbuehl, R. Langerm, Isolation, differentiation and characterization of vascular cells derived from human embryonic stem cells. *Nat. Protoc.* **5**, 1115–1126 (2010).
11. D. James, H.-s. Nam, M. Seandel, D. Nolan, T. Janovitz, M. Tomishima, L. Studer, G. Lee, D. Lyden, R. Benezra, N. Zaninovic, Z. Rosenwaks, S. Y. Rabbany, S. Rafii, Expansion and maintenance of human embryonic stem cell–derived endothelial cells by TGFβ inhibition is Id1 dependent. *Nat. Biotechnol.* **28**, 161–166 (2010).
12. V. V. Orlova, F. E. van den Hil, S. Petrus-Reurer, Y. Drabsch, P. ten Dijke, C. L. Mummery, Generation, expansion and functional analysis of endothelial cells and pericytes derived from human pluripotent stem cells. *Nat. Protoc.* **9**, 1514–1531 (2014).
13. N. Prasain, M. R. Lee, S. Vemula, J. L. Meador, M. Yoshimoto, M. J. Ferkowicz, A. Fett, M. Gupta, B. M. Rapp, M. R. Saadatzadeh, M. Ginsberg, O. Elemento, Y. Lee, S. L. Voytik-Harbin, H. M. Chung, K. S. Hong, E. Reid, C. L. O'Neill, R. J. Medina, A. W. Stitt, M. P. Murphy, S. Rafii, H. E. Broxmeyer, M. C. Yoder, Differentiation of human pluripotent stem cells to cells similar to cord-blood endothelial colony–forming cells. *Nat. Biotechnol.* **32**, 1151–1157 (2014).
14. X. Bao, X. Lian, K. K. Dunn, M. Shi, T. Han, T. Qian, V. J. Bhute, S. G. Canfield, S. P. Palecek, Chemically-defined albumin-free differentiation of human pluripotent stem cells to endothelial progenitor cells. *Stem Cell Res.* **15**, 122–129 (2015).
15. S. J. Arnold, J. Stappert, A. Bauer, A. Kispert, B. G. Herrmann, R. Kemler, *Brachyury* is a target gene of the Wnt/β-catenin signaling pathway. *Mech. Dev.* **91**, 249–258 (2000).
16. W. C. Dunty Jr., K. K. Biris, R. B. Chalamalasetty, M. M. Taketo, M. Lewandoski, T. P. Yamaguchi, Wnt3a/β-catenin signaling controls posterior body development by coordinating mesoderm formation and segmentation. *Development* **135**, 85–94 (2008).
17. S. Dupont, L. Morsut, M. Aragona, E. Enzo, S. Giulitti, M. Cordenonsi, F. Zanconato, J. Le Digabel, M. Forcato, S. Bicciato, N. Elvassore, S. Piccolo, Role of YAP/TAZ in mechanotransduction. *Nature* **474**, 179–183 (2011).
18. Y. Sun, K. M. A. Yong, L. G. Villa-Diaz, X. Zhang, W. Chen, R. Philson, S. Weng, H. Xu, P. H. Krebsbach, J. Fu, Hippo/YAP-mediated rigidity-dependent motor neuron differentiation of human pluripotent stem cells. *Nat. Mater.* **13**, 599–604 (2014).
19. C. Yang, M. W. Tibbitt, L. Basta, K. S. Anseth, Mechanical memory and dosing influence stem cell fate. *Nat. Mater.* **13**, 645–652 (2014).

20. T. P. Driscoll, B. D. Cosgrove, S.-J. Heo, Z. E. Shurden, R. L. Mauck, Cytoskeletal to nuclear strain transfer regulates YAP signaling in mesenchymal stem cells. *Biophys. J.* **108**, 2783–2793 (2015).
21. C. Yang, F. W. DelRio, H. Ma, A. R. Killaars, L. P. Basta, K. A. Kyburz, K. S. Anseth, Spatially patterned matrix elasticity directs stem cell fate. *Proc. Natl. Acad. Sci. U.S.A.* **113**, E4439–E4445 (2016).
22. S. Premaraj, I. Souza, T. Premaraj, Mechanical loading activates β-catenin signaling in periodontal ligament cells. *Angle Orthod.* **81**, 592–599 (2011).
23. L. Przybyla, J. N. Lakins, V. M. Weaver, Tissue mechanics orchestrate Wnt-dependent human embryonic stem cell differentiation. *Cell Stem Cell* **19**, 462–475 (2016).
24. S. Kusuma, Y.-I. Shen, D. Hanjaya-Putra, P. Mali, L. Cheng, S. Gerecht, Self-organized vascular networks from human pluripotent stem cells in a synthetic matrix. *Proc. Natl. Acad. Sci. U.S.A.* **110**, 12601–12606 (2013).
25. R. W. Style, R. Boltyanskiy, G. K. German, C. Hyland, C. W. MacMinn, A. F. Mertz, L. A. Wilen, Y. Xu, E. R. Dufresne, Traction force microscopy in physics and biology. *Soft Matter* **10**, 4047–4055 (2014).
26. X. Y. Chan, R. Black, K. Dickerman, J. Federico, M. Lévesque, J. Mumm, S. Gerecht, Three-dimensional vascular network assembly from diabetic patient-derived induced pluripotent stem cells. *Arterioscler. Thromb. Vasc. Biol.* **35**, 2677–2685 (2015).
27. S. Kusuma, E. Peijnenburg, P. Patel, S. Gerecht, Low oxygen tension enhances endothelial fate of human pluripotent stem cells. *Arterioscler. Thromb. Vasc. Biol.* **34**, 913–920 (2014).
28. R. McBeath, D. M. Pirone, C. M. Nelson, K. Bhadriraju, C. S. Chen, Cell shape, cytoskeletal tension, and RhoA regulate stem cell lineage commitment. *Dev. Cell* **6**, 483–495 (2004).
29. Z. Ma, J. Wang, P. Loskill, N. Huebsch, S. Koo, F. L. Svedlund, N. C. Marks, E. W. Hua, C. P. Grigoropoulos, B. R. Conklin, K. E. Healy, Self-organizing human cardiac microchambers mediated by geometric confinement. *Nat. Commun.* **6**, 7413 (2015).
30. M. P. Lutolf, P. M. Gilbert, H. M. Blau, Designing materials to direct stem-cell fate. *Nature* **462**, 433–441 (2009).
31. E. A. Vogler, Protein adsorption in three dimensions. *Biomaterials* **33**, 1201–1237 (2012).
32. L. Azzolin, T. Panciera, S. Soligo, E. Enzo, S. Bicciato, S. Dupont, S. Bresolin, C. Frasson, G. Basso, V. Guzzardo, A. Fassina, M. Cordenonsi, S. Piccolo, YAP/TAZ incorporation in the β-catenin destruction complex orchestrates the Wnt response. *Cell* **158**, 157–170 (2014).
33. A. J. Engler, S. Sen, H. L. Sweeney, D. E. Discher, Matrix elasticity directs stem cell lineage specification. *Cell* **126**, 677–689 (2006).
34. X. Lian, C. Hsiao, G. Wilson, K. Zhu, L. B. Hazeltine, S. M. Azarin, K. K. Raval, J. Zhang, T. J. Kamp, S. P. Palecek, Robust cardiomyocyte differentiation from human pluripotent stem cells via temporal modulation of canonical Wnt signaling. *Proc. Natl. Acad. Sci. U.S.A.* **109**, E1848–E1857 (2012).
35. J. A. Selekman, N. J. Grundl, J. M. Kolz, S. P. Palece, Efficient generation of functional epithelial and epidermal cells from human pluripotent stem cells under defined conditions. *Tissue Eng. Part C Methods* **19**, 949–960 (2013).
36. X. Lian, X. Bao, A. Al-Ahmad, J. Liu, Y. Wu, W. Dong, K. K. Dunn, E. V. Shusta, S. P. Palecek, Efficient differentiation of human pluripotent stem cells to endothelial progenitors via small-molecule activation of WNT signaling. *Stem Cell Rep.* **3**, 804–816 (2014).
37. A. Das, R. S. Fischer, D. Pan, C. M. Waterman, YAP nuclear localization in the absence of cell-cell contact is mediated by a filamentous actin-dependent, myosin II- and phospho-YAP-independent pathway during extracellular matrix mechanosensing. *J. Biol. Chem.* **291**, 6096–6110 (2016).
38. S. Kusuma, A. Facklam, S. Gerecht, Characterizing human pluripotent-stem-cell-derived vascular cells for tissue engineering applications. *Stem Cells Dev.* **24**, 451–458 (2014).
39. C. Patsch, L. Challet-Meylan, E. C. Thoma, E. Urich, T. Heckel, J. F. O'Sullivan, S. J. Grainger, F. G. Kapp, L. Sun, K. Christensen, Y. Xia, M. H. C. Florido, W. He, W. Pan, M. Prummer, C. R. Warren, R. Jakob-Roetne, U. Certa, R. Jagasia, P.-O. Freskgård, I. Adatto, D. Kling, P. Huang, L. I. Zon, E. L. Chaikof, R. E. Gerszten, M. Graf, R. Iacone, C. A. Cowan, Generation of vascular endothelial and smooth muscle cells from human pluripotent stem cells. *Nat. Cell Biol.* **17**, 994–1003 (2015).
40. B.-K. Chou, P. Mali, X. Huang, Z. Ye, S. N. Dowey, L. M. S. Resar, C. Zou, Y. A. Zhang, J. Tong, L. Cheng, Efficient human iPS cell derivation by a non-integrating plasmid from blood cells with unique epigenetic and gene expression signatures. *Cell Res.* **21**, 518–529 (2011).
41. Y.-T. Wu, I.-S. Yu, K.-J. Tsai, C.-Y. Shih, S.-M. Hwang, I.-J. Su, P.-M. Chiang, Defining minimum essential factors to derive highly pure human endothelial cells from iPS/ES cells in an animal substance-free system. *Sci. Rep.* **5**, 9718 (2015).
42. X. Liu, J. Qi, X. Xu, M. Zeisberg, K. Guan, E. M. Zeisberg, Differentiation of functional endothelial cells from human induced pluripotent stem cells: A novel, highly efficient and cost effective method. *Differentiation* **92**, 225–236 (2016).

Acknowledgments: We would like to thank L. Cheng for provision of the hiPSC line; H. Jones and A. Jones for technical assistance; and M. Blatchley, B. Macklin, and D. Lewis for productive discussions throughout this work. We would also like to thank S. Marra and Z. Xia for their assistance in characterizing the mechanical properties of the PDMS substrates and S. Sun's group for the provision of the 3-kPa substrates. **Funding:** This work was supported by the NSF Graduate Research Fellowships Program (DGE-1232825 to Q.S.); NIH/National Heart, Lung, and Blood Institute [F31HL134329 (to Q.S.) and F32HL128038 (to X.Y.C.)]; and American Heart Association (15EIA22530000), NSF (1054415), Maryland Stem Cell Fund (MSCRFI-2784), the W.W. Smith Charitable Trust award (H1302), and the President's Frontier Award from Johns Hopkins University (to S.G.). **Author contributions:** Q.S., X.Y.C., A.M.C., M.S., and S.G. designed the research; Q.S., X.Y.C., A.M.C., M.T., and M.S. performed the research; Q.S., X.Y.C., A.M.C., and S.G. analyzed the data; and Q.S., X.Y.C., and S.G. wrote the paper. **Competing interests:** S.G. is a cofounder and was a consultant at Gemstone Biotherapeutics LLC. The other authors declare that they have no competing interests. **Data and materials availability:** All data needed to evaluate the conclusions in the paper are present in the paper and/or the Supplementary Materials. Additional data related to this paper may be requested from the authors.

Submitted 18 November 2016
Accepted 10 April 2017
Published 31 May 2017
10.1126/sciadv.1602883

Citation: Q. Smith, X. Y. Chan, A. M. Carmo, M. Trempel, M. Saunders, S. Gerecht, Compliant substratum guides endothelial commitment from human pluripotent stem cells. *Sci. Adv.* **3**, e1602883 (2017).